Local cluster formation in a cobalt melt during the cooling process

Li Hui,[1,2,*] Wang Guanghou,[1] Bian Xiufang,[3] and Ding Feng[1]
[1]*National Laboratory of Solid State Microstructures of Nanjing University, Nanjing, P. R. China 210093*
[2]*Mechanical Department, Shandong Institute of Technology, Zibo, P. R. China 255012*
[3]*The Key Laboratory of Liquid Structure and Heredity of Materials, Ministry of Education, Shandong University, Jinan, P. R. China 250061*

(Received 11 April 2001; revised manuscript received 2 July 2001; published 26 December 2001)

Investigations of the thermal evolution of the structural and dynamic properties of small cobalt clusters in melt are performed using molecular-dynamics simulations with a Finnis-Sinsclaire potential. The mean square displacements, atomic volume, and internal energy, as well as the pair correlation function and bonded pairs, are obtained from quick and slow cooling simulations, respectively. The splitting of a second peak of pair correlation function is due to the presence of icosahedron-type clusters. The results demonstrate that the transition from a supercooled-liquid to a crystal is a discontinuous transition in structure, while the supercooled-liquid to glass transition is a continuous transition in structure. The physical picture of the structure of metallic glass is a disordered entanglement with a lot of icosahedra.

DOI: 10.1103/PhysRevB.65.035411 PACS number(s): 64.70.Dv

I. INTRODUCTION

When a liquid is cooled, it can solidify in two very different ways. The familiar route produces an ordered crystal with long-range order. In this case, the change in the mechanical properties of the materials from viscous liquid to elastic solid can easily be explained by the change in structure. An equally important but subtle transformation is disordered glass without long-range order. Understanding a transition from a supercooled-liquid to a solid (crystal and glass) is an important practical issue in physical sciences. Some important questions on about freezing have remained unanswered. Experiments have not allowed us to measure directly how an atom moves to a particular neighbor in a solid or to observe which local structures are prone to reorganization. Therefore, a liquid-to-solid transition determined by experiment is hardly possible. Computer simulations provide an opportunity to study these processes at an atomic level. In the past 20 years, there has an upsurge of interest in understanding the liquid-to-solid transition.[1–10] In a structural analysis, the pair correlation function is no doubt of the chosen value. It yields the central information about the short-range order, and serves as a key test for different structure models.[11] To study the pair correlation function as well as thermodynamic properties, theoretically two distinct techniques of computer simulation, namely, the molecular-dynamics and Monte Carlo methods, are most frequently employed. In both techniques, the interaction potential is the primary input for computation. Mitral and co-workers[12,13] have used a two-body model with Coulombic interactions and a power-law repulsion, fitted to the short-range structure and melting temperature of cristobalite. Three-body forces have been introduced mainly to bring the bond angle distributions into better agreement with the experimental data for the glass.[14] An optimized two-body potential developed by Tsuneyuki was applied with success to a study of a thermal-induced phase transition in crystalline silica.[15] The effective pair potential was used to study the microstructure of amorphous Cr and Ga metals.[16,17] A molecular-dynamics simulation was used to simulate not only the glass formation processes but also crystallization processes from the liquids. Stillinger and Laviolett reported local order in quenched states of simple atomic substances.[18] Watanabe and Tsumurava studied the crystallization and glass formation in liquid sodium by the molecular-dynamics (MD) method.[19] The homogeneous nucleation of the crystalline phase from a supercooled liquid phase was studied for several model systems by means of the molecular-dynamics simulation. Hsu and Rahman reported homogeneous nucleation and growth of a fcc crystalline phase with Lennard-Jones (LJ) 12-6 systems.[20] Several other fcc crystallization phase was observed in soft core[21,22] and rubidium.[23] Moutain and Brown reported an observation of the body-centered-cubic (bcc) structure in a LJ.[24] Hsu and Rahman system is observed the homogeneous nucleation and growth of a bcc structure in rubidium systems.[25] Analyses was made of the size of the critical nucleus,[20] the structural feature of the nucleation,[21,22] the effects of the types of potential,[24] and the effects of boundary conditions.[20] However, the simulated results mentioned above can only be used to demonstrate the temperature effects on the structure-dependent part of the energy. The transition from a liquid to a solid is investigated only by specific-heat or thermodynamics properties. It is interesting to study how the local cluster changes when a transition from a liquid to a solid occurs. However, till now, results in this research field have been insufficient. Moreover, a study of the transition from a supercooled liquid to a solid with many-body potential was scarcely reported. In the present study, the transition from a supercooled liquid to a solid (glass and crystal) is simulated by means of the Finnis-Sinsclaire (FS) potential. We will simulate the cooling process of the liquid cobalt with three cooling rates. In Sec. II, the FS potential is described in detail. In Sec. III, we will describe the computational procedures and cooling method. In Sec. IV, a structural analysis will be introduced. Our simulated results and discussion will be given in Sec. V. Concluding remarks will be given in Sec. VI.

II. INTERATOMIC POTENTIAL

In an atomistic modeling of transition metals, pair potentials have been found to be insufficient to explain a number of observations. In recent times, the FS potential[26] was presented for deriving empirical *N*-body interatomic potentials for atomistic simulations which are more realistic than pairwise interactions between atoms, and reasonably fast in computation. The schemes can be regarded as a version of the so-called embedded-atom method which was developed by Daw and Baskes.[27] The *N*-body potentials developed by FS were used successfully to study the point defect properties in Ni_3Al (Ref. 28) and surface.[29–31] The FS potential also led to encouraging results in a number of atomistic studies in cubic transition and noble metals.[32,33] Igarashi, Khanta and Vitek used the FS potential to calculate the phonon dipersion relations for [110], [100], and [001] directions in the Brillouin zone of the cobalt. They are in a good agreement with experiments, indicating that the FS potential is good enough to describe the cobalt.[34] The FS potential formalism is based on a second-moment approximation to the tight-binding theory, assuming that the change in shape of the *d*-band induced by the local environment can be represented as a simple compression of band-width and that there is no charge transfer between atoms. The total energy of *N* interacting particles is written as[34]

$$E_{\mathrm{tot}}=\frac{1}{2}\sum_{ij} V(r_{ij})-\sum_{i} f(\rho_i),$$

$$\rho_i=\sum_{j} \phi(r_{ij}),$$

where the summation extends over all the atoms, $V(r_{ij})$ is a pair potential describing a direct interaction between two atoms i and j separated by a distance r_{ij}, which is strongly repulsive for small separations of atoms; f is taken as a square-root function; ρ_i is interpreted as a sum of square hopping integrals; and $\phi(r_{ij})$ is another pair potential.

The first and second derivatives of the functions $V(r)$ and $\phi(r)$ should be continuous for all values of r, and the following forms adopted for the most convenience

$$V(r)=\sum_{k=1}^{n} A_k(R_{ak}-r)^3H(R_{ak}-r),$$

$$\phi(r)=\sum_{k=1}^{m} B_k(R_{bk}-r)^3H(R_{bk}-r),$$

$$H(x)=\begin{cases}0, & x<0\\ 1, & x>0,\end{cases}$$

where $H(x)$ is Heaviside unit-step function which gives the cutoff distance of each spline segment; x represents $R_{bk}-r$ or $R_{ak}-r$; m and n are the numbers of knot points for $\phi(r)$ and $V(r)$, $m=4$ and $n=6$; R_{ak} and R_{bk} are chosen knot points such that $R_{a1}>R_{a2}>\cdots R_{an}$ and $R_{b1}>R_{b2}>\cdots R_{bm}$; the coefficients A_k and B_k are determined by fitting the experimental quantities. The parameters of the FS potential for some hexagonal close packed (HCP) metals are summarized in Table I.[34]

TABLE I. The parameters of FS potential for cobalt, R_{ak} and R_{bk} are chosen knot points, and coefficients A_k and B_k are determined by fitting the experimental quantities.

	$V(r)$		$\Phi(r)$
R_{a1}	1.801 400 0	R_{b1}	1.880 000 0
R_{a2}	1.732 050 8	R_{b2}	1.623 451 2
R_{a3}	1.623 400 0	R_{b3}	1.411 449 7
R_{a4}	1.411 449 7	R_{b4}	1.025 000 0
R_{a5}	1.205 724 8	B_1	7.143 128 6
R_{a6}	1.025 000 0	B_2	−12.929 982 1
A_1	0.994 817 6	B_3	−7.752 371 2
A_2	0.215 630 9	B_4	1349.226 977
A_3	−2.098 957 7		
A_4	−1.499 356 6		
A_5	0.475 308 3		
A_6	236.986 365 9		

III. MD SIMULATION PROCESS

The computer liquids and solids (crystals and glasses) of cobalt are simulated by MD techniques using the damped force method[35–38] at a constant pressure. The velocity rescaling algorithm is employed to control the temperature. A simple method of fixing the kinetic temperature of a system in MD is to rescale the velocities at each time step. The damped force method involves the integration of a modified set of Hamiltonian equations of motion. A kind of friction coefficient is chosen to constrain equations of motion. Thus, for the ''leapfrog'' algorithm, the damped force method reduces to a simple scaling of the velocities and the forces at each integration step. It ensures that temperature is constant at every time step. Here a MD simulations is carried out in a cubic box subject to widely used periodic boundary conditions with 500 particles. The time step is chosen at 5×10^{-15} sec. The equation of motion is integrated using the velocity verlet algorithm. In order to obtain melting liquid state, the simulations started at 1873 K. At this temperature, the system is run for 3×10^6 time steps to guarantee an equilibrium liquid state. Then the damped force method is adopted to decrease the temperature with cooling rates are 4×10^{13}, 4×10^{11}, and 4×10^{10} K/s respectively by forcing the bath temperature to decrease linearly at every time step. The configurations are recorded at particular temperatures during the quenching. For each of the recorded configurations, another run of 3×10^6 time steps at the given temperature is performed in order to determine the thermodynamic quantities. During each of these runs, 20 configurations are saved, one at each 2000 time steps. Also the steepest decent energy-minimization procedure with the conjugate gradient method, suggested by Stillinger and co-workers,[39,40] is imposed on each of these configurations to extract their inherent configurations, in which atoms are brought to local mini-

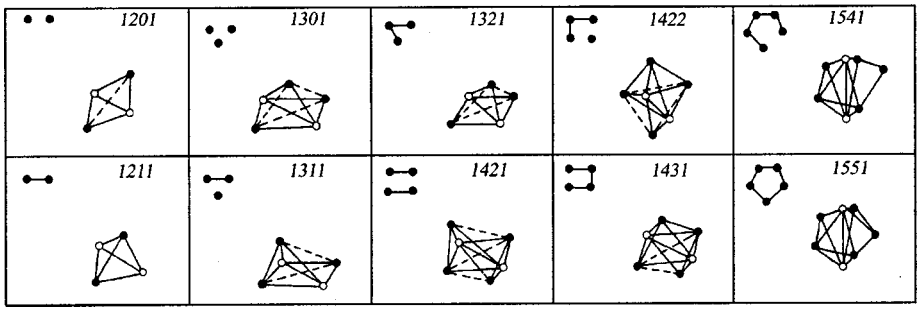

FIG. 1. The schematic diagram for some bonded pairs.

mum on the potential-energy surface. This procedure was used extensively as a very powerful means of analyzing the structure of liquids, amorphous solids, and even crystals.[41,42] It is presumed that the analysis of inherent structure of a material can provide a clearer picture of its structure because the inherent structure does not contain instantaneous high-energy fluctuations that are present in the actual dynamical state and thus obscure our observation.

IV. STRUCTURAL ANALYSIS METHODS

An additional strategy involves monitoring the mean square displacements (MSD's) of atoms from their initial positions. This function increases during the course of a liquid simulation, but oscillates around a mean value in a solid. A useful rule of thumb is that when the root-mean-square displacement per particle exceeds a value of 0.5σ and it is clearly increasing, then the system has melted and the equilibration can be terminated. Care should be taken to exclude periodic boundary corrections in the computation of this quantity. This technique is very useful for monitoring equilibration not only from a lattice but also from a disordered starting configuration, particularly when the system may become trapped in a glassy state rather than forming a liquid, that would be interesting for these case. The displacement MSD is given by:[43,44]

$$\langle r^2(t)\rangle = \frac{1}{N}\sum_{i=1}^{N}[r_i(t)-r_i(0)]^2.$$

The MSD is proportional to the diffusion constant D,

$$D = \frac{1}{6}\frac{d}{dt}\langle r^2(t)\rangle,$$

where N is the particle number and $r(t)$ is the position at time t, $r(0)$ is the position at the time origin. A nonzero value of D is suggestive of a liquid. It is a necessary but sufficient criterion for liquidlike behavior.

The structure of a liquid is characterized by a set of distribution functions, the simplest one being the pair correlation functions. This function gives the probability of finding a pair of atoms a distance r apart, relative to the probability expected for a completely random distribution at the same density. The pair correlation function is determined from[45]

$$g(r) = \frac{\Omega\langle n_i(r,r+\Delta r)\rangle}{4\pi r^2 \Delta r N}.$$

Here $\langle n_i(r,r+\Delta r)\rangle$ is the average number of atoms surrounding the ith atom in a spherical shell between r and $r+\Delta r$. N is the total number of atoms involved in the system under consideration, and Ω is the simulated volume of the unit cell. The pair correlation function is frequently used for discussions of noncrystalline and crystal systems. The information given by the pair correlation function is only one dimensional, but it does give quantitative information about liquid, crystalline, and noncrystalline systems. Therefore, the pair correlation function is one of the most important pieces of information in the study of such materials. The pair correlation function is useful, not only because it provides insight into the liquid and solid structures, but also because the ensemble average of any function may be expressed in this form. For example, we may write the energy as

$$E = \frac{3}{2}Nk_BT + 2\pi n\rho\int_0^\infty r^2\nu(r)g(r)dr.$$

To analyze the structural changes accompanying freezing, we adopt a common technique used by Anderson and co-workers.[46,47] In this technique, two atoms are said to be near neighbors if they are within a specified cutoff distance of each other. The graphical shorthand provides a convenient way to represent the possible type of atomic pairs (Fig. 1). Here the diagrams represent physical structures rather than integrals. In a particular diagram, white points represent atoms in the root pair, while black points represent near neighbors with these atoms in common. Atoms that are near neighbors of each other are connected by lines (bonds). Note that two white points appear in every diagram of this type, and that, based on the definition, each white point is bonded to each black point. We can characterize each of the diagrams by a sequence of four integers. The first integer, either 1 or 2, indicates the diagram ''type,'' that is, whether or not the atoms composing the root pair are near neighbors. The second integer represents the number of near neighbors shared by the root pair. The third integer denotes the number of bonds among the shared neighbors. A fourth integer, whose value is arbitrary as long as it is used consistently, is added to provide a unique correspondence between the number and the diagram. Figure 1 shows some diagrams that are prevalent in the system. Each of the various phases of dense bulk system has its own signature in the diagrams that characterize its local structures. For example, four diagrams are represented in a perfect bulk fcc crystal: 2211, 2101, 1421, and 2441. A bulk hcp crystal contains 1422 and 2331 pairs. The 1421 and 1422 pairs are less abundant in a random closed-packed glass

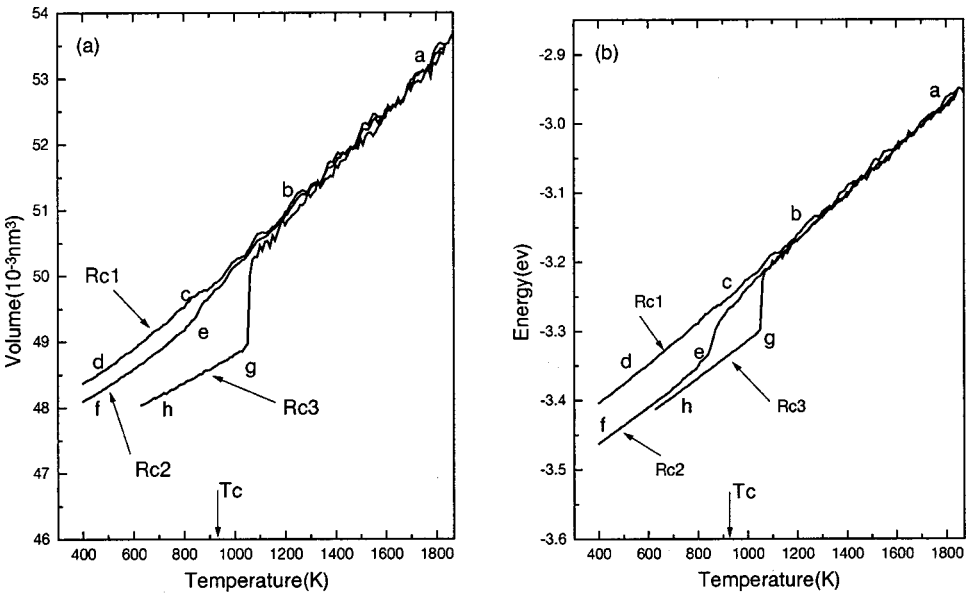

FIG. 2. The atomic volume (a) and internal energy (b) vs the temperature during the cooling process ($R_c1{:}4\times10^{13}$ K/s; $R_c2{:}4\times10^{11}$ K/s; $R_c3{:}4\times10^{10}$ K/s).

system, and 1551 and 1541 pairs, which are not present in perfect fcc or hcp crystals, are relatively numerous in supercooled liquid and glasses. Mackay icosahedra contain some 1551 pairs, not present in either fcc or hcp crystals. A large Mackay icosahedron is, however, composed of twined, distorted fcc tetrahedron. Types of pairs not found in fcc systems can appear only where these tetrahedra meet. In fact, the 1551 cluster is a decahedron. It is necessary to point out that the 1551 and 1541 clusters are used to directly measure the icosahedral order in the liquid. The 1421 cluster is the typical pair of a fcc crystal. The 1661 and 1441 clusters are the characteristic pairs of bcc crystal. The 1421 and 1422 clusters are related to the HCP crystal. The 1201 and 1311 clusters represent the rhombus symmetrical features of the short-range position order.

Pair analyses or systems are performed in a separate program. The information on the statistical occurrence of different structural units is obtained by averaging over the 20 inherent configurations recorded in the above MD runs. If the distance of two atoms (a pair) is smaller than a given cutoff distance, chosen to be equal to the position of the first minimum in the appropriate pair correlation function, then such atoms are referred to as neighbors or, equivalently, are considered to form a bond. With the Honeycutt-Andersen pair analysis technique, the statistical occurrence of local structural units can be obtained easily at the atomic level by computer simulation.

V. RESULTS AND DISCUSSION

We now turn to a numerical examination of the applicability of the above-described MD simulation. The present simulation is carried out for pure cobalt metal. The results obtained using various cooling rates (i.e., $R_c1=4\times10^{13}$ K/s, $R_c2=4\times10^{11}$ K/s, and $R_c3=4\times10^{10}$ K/s) for the corresponding internal energy $E(t)$ and mean atomic volume $\Omega(t)$ are displayed in Fig. 2. In Fig. 2, the *abcd* line represents $\Omega(t)$ for a pure cobalt metal quenched with a fast cooling rate (4×10^{13} K/s), whereas the *abef* and *abgh* lines denote $\Omega(t)$ for pure cobalt quenched with a much lower cooling rate (4×10^{11} and 4×10^{10} K/s). In fact, the former and the latter lines represent the Ω-t relation for a transition from a metallic supercool liquid to a glass, and that for a transition from a metallic supercooled liquid to a hcp crystal respectively. At a temperature somewhat above the crystal-transition temperature in Fig. 2, the cooling dependence of the calculation becomes important, and hence the *ab* line splits into three lines with further decreases in T, shown in Fig. 2. As we know, the value of the melting temperature of cobalt is 1768 K. However, because the transition point T from a supercooled liquid to a crystal is affected greatly by the cooling rates, the transition point T is lower than the true melting temperature of Co. We know from Fig. 2 that the transition point T at R_c3 is closer to the true melting temperature than that at R_c2. We can conclude that if the cooling rate is slow enough the transition temperature is approximately for true melting point. At the cooling rate as 4×10^{13} K/s used in these runs, the energy and the atomic volume have no break with decreasing temperature. This means that the system is frozen into glass. By contrast, at a cooling rate of 4×10^{11} K/s, the internal energies and atomic volume undergo a sharp freezing transition when the temperature decreases, demonstrating that a phase transition occurs and some clusters are frozen into crystal structures. These two different results come from the different cooling rates. At a slow cooling rate, atoms in the liquid have enough time to move their equilibrated position to form a crystal, whereas the rapid cooling rate restricts the atom diffusion and prevent crystallization.

The results for MSD's and temperature T are shown in Fig. 3(a). At a cooling rate of 4×10^{11} K/s, MSD increases with decreasing temperature. When the temperature is low enough, the MSD no longer increases, implying that the system is in thermal equilibrium. But, however at a cooling rate of 4×10^{13} K/s, the MSD does not significantly change with decreasing temperature. This result suggests that the high cooling rate may restrict the atomic diffusion. Having deter-

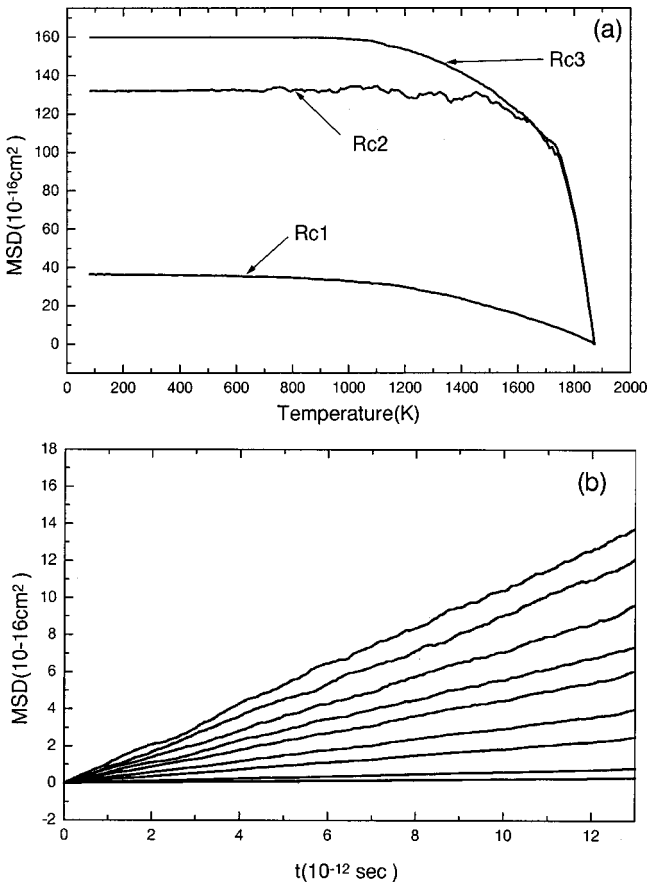

FIG. 3. mean-square displacement of Co vs the temperature and time curves *a* are the MSD-temperature curves, $R_c1{:}4\times10^{13}$ K/s; $R_c2{:}4\times10^{11}$ K/s; $R_c3{:}4\times10^{10}$ K/s. Curves *b* are the MSD-time curves. Curves from top to bottom correspond to the temperature $T(K)=1873$, 1720, 1570, 1420, 1270, 1120, 970, 520, and 300 respectively.

mined $\Omega(t)$ and $E(t)$, involved in the transition from a liquid to a glass or crystal, the time dependence of the atomic mean-square displacement [MSD(t)] can be calculated immediately[48] by performing another run of 3×10^6 time steps from the atomic configurations recorded at each particular temperature in the present MD simulation on both $\Omega(t)$ and $E(t)$. The results thus obtained for the MSD(t) are displayed in Fig. 3(b). The slope of the MSD curve is proportional to the diffusion coefficient, and is a useful measure of the mobility of the constituent particles. There are two aspects of the displayed results that merit emphasis. First, for temperature between T_m and T_c, the MSD always increases with time, consistent with the generalized Einstein model in which the atom in a cage, formed by its surrounding atoms, oscillates about a center which itself is undergoing Brownian motion.[49] The high-lying MSD curves may be interpreted by means of a free-volume-like model. At high temperature all of the atomic cages in the supercooled cobalt liquid become unstable due to the strong thermal effects on the atoms and, as a result, some of the atomic cages break, and atoms initially enclosed in these cages may move according to a Langevin-type equation. Second, in going down from T_c to a low T, the slope of the MSD(t) curve tends to vanish. Because at low temperature the cages become localized, the involved atoms tend to cease their diffusive motion. Accordingly, the supercooled-liquid region from T_m to T_c for pure cobalt metal consists of two different structural regimes, namely, an undercooled region from T_m to $T=0.65T_m$ and a high hypercooled region from $T=0.65T_m$ to T near T_c. Note that pure cobalt metal must be less disordered in the hypercooled region than that in the undercooled region, because the creation and annihilation of atomic cages occurs in the undercooled region but not in the hypercooled region where the atomic cages are rather stable. To proceed further, we now examine the corresponding structural properties.

The structure of the simulated liquids is conveniently discussed in terms of the pair correlation function (PCF). Figure 4 shows the PCF as a function of temperature. To check the accuracy of the FS potential, the theoretical pair correlation function is compared with experimental result obtained by Waseda.[50] The theoretical values are merely in good agreement with the corresponding experimental result at 2023 K, implying that the presently used FS potential is highly accurate for the present study. The overall agreement between simulation and experiment is rather good. Turning to Fig. 4(a), at a cooling rate of 4×10^{13} K/s, we note that all of the principal structural features of an amorphous solid are clearly seen. The second peak splitting is characteristic feature of amorphous formation. The splitting of the second peak in the PCF, for conventional rapidly quenched metals into two subpeaks is due to the presence of icosahedron-type clusters. It is also interesting to note that the structure of the amorphous state develops progressively as the temperature quench becomes greater. The transition from a supercooled liquid to a glass is a continuous transition in structure. The result is threefold: (i) the first peak becomes more and more pronounced in magnitude, accompanied by narrowing in the width; (ii) the second peak flattens in shape and eventually, at room temperature, fully develops into a distinct double-peak splitting; and (iii) the amplitudes of the oscillations are larger at lower temperature for peaks beyond the second one. From the results we know that the shapes of the pair correlation functions at 300 and 1873 K are rather alike, suggesting a structural similarity between the glass and the liquid. Contrary to the atomic distribution in both gaseous and liquid states, it is probable that the positional change of atoms is relatively limited in the amorphous state. It should be noted that this difference has an influence on the formation of a characteristic structure for the amorphous state, although the basic arrangement of atoms in the amorphous state is similar to that in the liquid state. In both liquid and amorphous states, the atoms are randomly distributed in a nearly closed-packed structure, and the mean free path is short and comparable to the atomic size. This implies that the positional correlation of atoms is relatively strong within the near-neighbor region. However, the average atomic configuration in the liquid state is more homogeneous than that of the amorphous state, because the atomic vibration is high. In other words, the atomic configuration in the amorphous state has more rigid packing than that of the liquid state. As a result, the average atomic distribution in the amorphous state shows a slight inhomogeneity, which frequently gives a de-

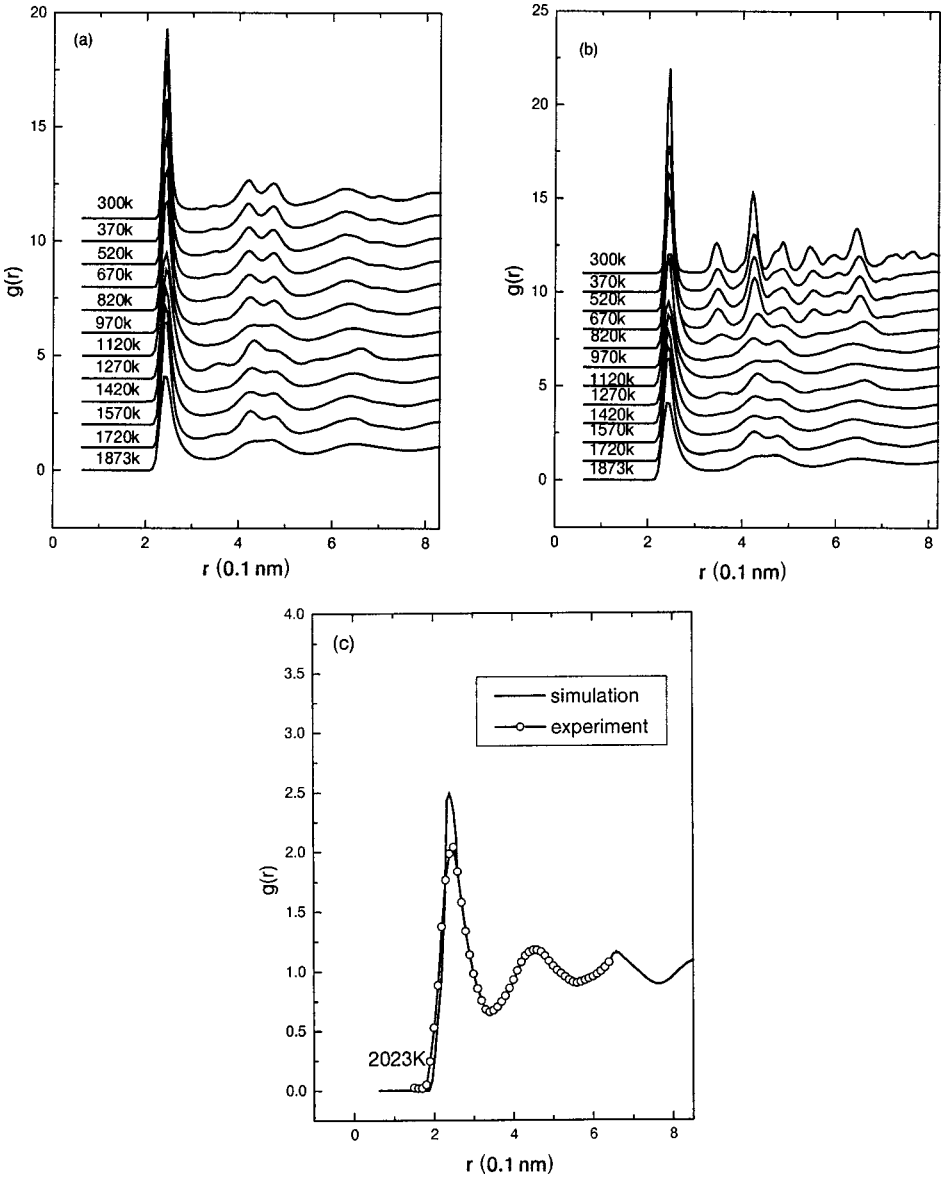

FIG. 4. The pair correlation functions for several temperatures. Curve *a*: $R_c1=4\times10^{13}$ K/s. Curve *b*: $R_c2=4\times10^{11}$ K/s. Curve *c*: comparison between simulation and experiment results.

formed pattern in the pair correlation function. In the crystalline state, the atoms occupy the cube corners of a regular three-dimensional lattice. Reflecting these characteristics, a series of growing dynamic pair correlation functions are shown on the right-hand side of Fig. 4(b). At a slow cooling rate 4×10^{11} K/s, the system produces some sharp multipeaks that are characteristic features of crystal formation: this result corresponds to the results of $\Omega(t)$ and $E(t)$ curves. As the temperature quench becomes greater, the crystal structure has developed progressively. The transition from a supercooled liquid to a crystal is a discontinuous transition in structure. This is a first-order-like transition that is confirmed by the result of Fig. 2. We also know from the result of Fig. 4(b) that before the crystal formation, the system is in supercooled liquid state, which is confirmed by the splitting second peak of pair correlation function. This result shows that the crystal results from a supercooled liquid through a proper cooling process. At the slow cooling rate 4×10^{11} K/s, the system has a long-range order feature in the final state. Conversely, the amorphous has short-range order feature. The two quenched structures indicate that different cooling rate would lead to different microstructure and cluster in system.

The PCF is a very important parameter to describe the structure of liquid. However, it is only a statistical average for all configurations of system. A lot of local structural information might be ignored. For example, all the fcc, ICOS, and hcp types clusters have 12 neighboring atoms. In other words, their coordination numbers are same but their symmetry is totally different. In order to characterize the local symmetry of clusters, the bond pair analysis is introduced in this paper. By means of the Honeycutt-Anderson pair analysis technique, the microscopic local structures of different kinds of clusters including the fivefold symmetry ones can be describe precisely at the atomic level. The results obtained in this application are summarized in Fig. 5. In this figure, 1441 and 1661 bonded pairs are characteristic of a bcc crystalline structure. The 1551 atomic bonded pair is characteristic of an icosahedral structure, which may appear in a noncrystalline system. 1421 and 1422 bonded pairs are characteristic of a

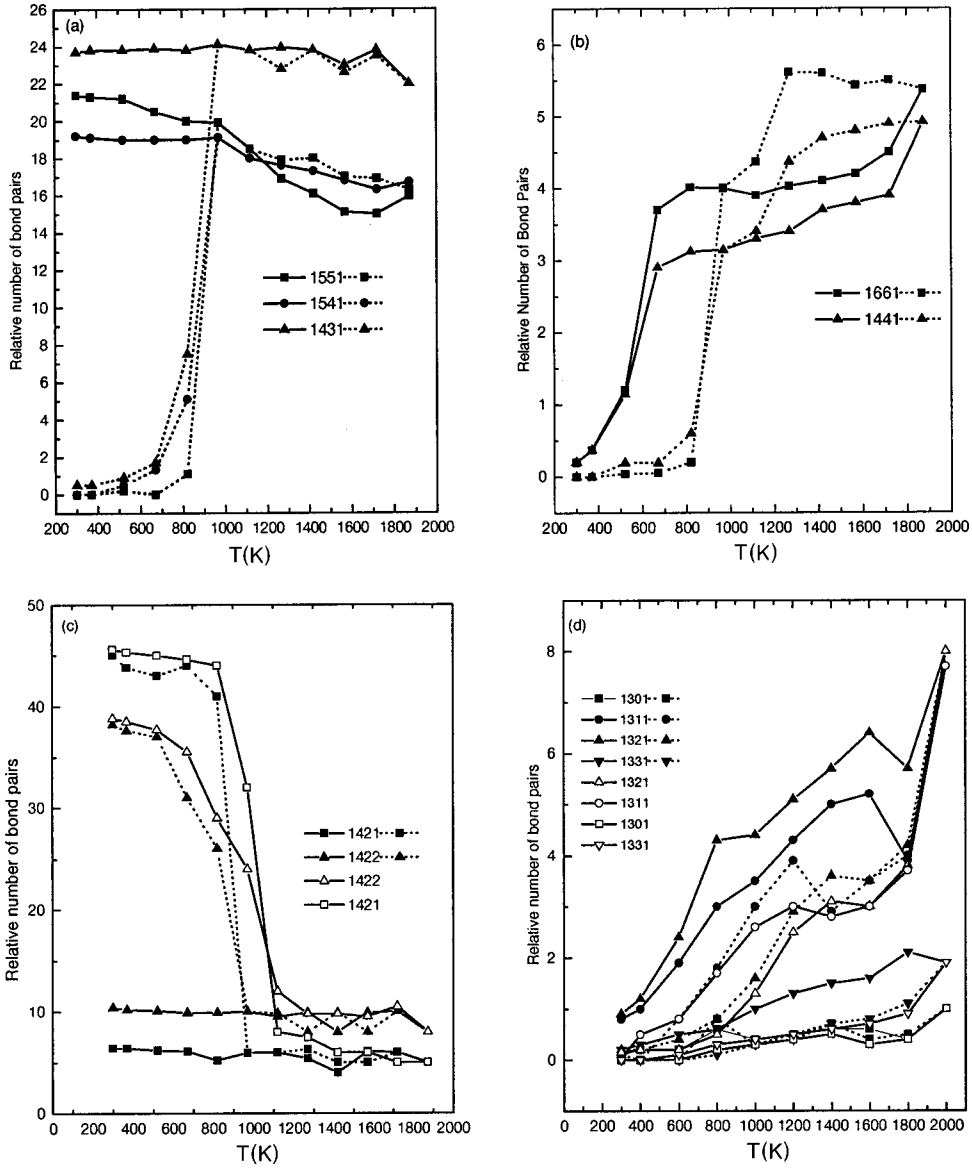

FIG. 5. The relative number of various bonded pairs for several temperatures. Curve *a*: 1551, 1541, and 1431. Curve *b*: 1661 and 1441. Curve *c*: 1421, and 1422. Curve *d*: 1331, 1321, 1311, and 1301. Solid line: $R_c1=4\times10^{13}$ K/s. Dashed line: $R_c2=4\times10^{11}$ K/s. Open symbol: $R_c3=4\times10^{10}$ K/s.

hcp crystalline structure. Since the 1551 cluster has a fivefold symmetry, the ratio of the 1551 cluster is a direct measurement of the degree of icosahedral order. The results in Fig. 5 show that the number of 1551 and 1541 clusters corresponding to icosahedra increases rapidly as the temperature decreases, at the faster cooling rate R_c1. Moreover, a large number of 1431 clusteróexist in liquid. The temperature does not change the amount of 1431 clusters during the cooling process. At low temperature, these three types of clusters reach to about 60% among all kinds of clusters. The 1551, 1541, and 1431 clusters are the major structures in liquid system. During the quick cooling process, the ratio of 1421 cluster associated with a hcp crystalline dose not change sensitively as the temperature decreases. Similar to a 1421 cluster, the ratio of the 1422 cluster also does not change significantly. This result implies that hcp unit is not sensitive to the temperature under the quick cooling condition. At low temperature, the ratio of two types of clusters only reaches up to 15% at a faster cooling rate R_c1. In Fig. 5, the increase in the cooling rate is found to have a much stronger effect on the number of small cluster such as 1551, 1541, 1431, 1422, and 1421. In the case of a slower cooling rate R_c2, the number of 1551, 1541, and 1431 clusters decrease dramatically and approach to zero at 300 K. For comparison, the number of 1421 and 1422 clusters corresponding to a hcp crystal increase rapidly by 45 and 38, respectively. It is interesting to note that, no matter which cooling rate is applied, both 1661 and 1441 clusters corresponding to a bcc crystal structure decrease rapidly with decreasing temperature. Similar to the R_c2 rate at a slower cooling rate R_c3 the supercooled liquid to crystal transition also occurred in a cobalt system. We know from Fig. 5 that the structural transition point at the cooling rate R_c3 is higher than that at the cooling rate R_c2. From 1873 to 1120 K, the number of 1421 and 1422 bond

pairs show no big changes, but at 970 K the number of 1421 and 1422 bond pairs have sudden increases, which means a structural transition occurs. It must be pointed out that the percent ratio of 1421 and 1422 bond pairs at the final temperature has no significant changes. At the cooling rate R_c3, some clusters in the system have enough time to regroup and form 1421 and 1422 bond pairs, so the transition temperature is much higher and close to the true melting temperature. On the other hand, at the cooling rate R_c2, because of the quick cooling rate some clusters in the system do not have enough time to reconstruct 1421 and 1422 bond pairs; the transition temperature is thus lower than at R_c3. When the cooling rate R_c1 is applied, the quick cooling rate R_c1 results in glass formation. Figure 5(d) shows that no matter which cooling rate is applied, the amounts of 1331, 1321, and 1301, clusters decrease with decreasing temperature. This result further supports that the degree of ordering of a liquid is enhanced with decreasing temperature. It is noted from Fig. 5d, that at the same temperature point, the number of bond pairs such as 1331, 1321, and 1301 at R_c3 is less than that at R_c2. This result further supports that, at R_c2, 1331, 1321, and 1301 bond pairs have chance to reconstruct and/or convert to 1421 and 1422 bond pairs relating to the hcp crystal. At two different cooling rates, it now turns out that the microstructure of the metal under consideration changes gradually from a liquid to a glass, as compared with the crystal-transition case, in which the values of N_{ijkl} change abruptly at T_c. Accordingly, the transition from a supercooled liquid to a glass is a continuous transition in structure, whereas the transition from a supercooled liquid to a crystal is discontinuous in structure. The change in the structure of a metallic system in the crystal transition from a supercooled-liquid state (which is metastable) is similar to that in the crystal transition form for the normal liquid state (which is stable); hence a transition from a supercooled liquid to a crystal would be a first-order-like transition. This is also illustrated by the sharp changes in both $\Omega(t)$ and $E(t)$ at T_c. At a quick cooling rate R_c1, it appears from Fig. 5 that the relative number of 1551 bonded pair continuously increase along with a corresponding decrease in the number of the 1421 and 1422 atomic bonded pairs when the temperature decreases. We mentioned above that the splitting of the second peak in the PCF for conventional rapidly quenched metals is due to the presence of icosahedron-type clusters. It is worth noting that the 1551 bonded pair is characteristic of an icosahedron-type cluster. Many 1551 bonded pairs appeared in glass, corresponding to a splitting of the second peak in the PCF. At the slow cooling rate R_c2, the relative numbers of 1551 and 1541 bonded pairs continuously decrease along with a sudden increase in the number of the 1421 and 1422 bonded pairs at T_c. In a conventional rapidly quenched metallic liquid, such as a cobalt liquid, the most prevalent atomic bonded pairs are of 1551 type rather than a 1421 and 1422 types. During the process of a transition from a supercooled liquid to a crystal, the 1551-, 1541-, and 1431-type clusters convert to 1421 and 1422 atomic bonded pairs, which are characteristic of some stable crystalline structure. It is worth mentioning that the relative numbers of the 1421 and 1422 bonded pairs an sensitive to the cooling rate.

It must be pointed out that only the 1551 cluster is regarded to have an ideal fivefold symmetry in the present study. Although a 1541 cluster has five neighbors in common, these five neighbors have only four bonds, the distance between two of the five neighbors's always beyond the cutoff distance of the first shell of the central atom; thus the 1541 cluster can be viewed to have a distorted fivefold symmetrical structure. Therefore, Voronoi statistics, using a simple number of the face, cannot distinguish a difference between 1551 and 1541 pairs. Experiment facts state that glass is a random-close-packed structure, and that it contains a many icosahedral structures. In fact, numerical results obtained by MD are in agreement with the experiment results. Honeycutt and Anderson gave us an opportunity to precisely define an icosahedron FK, and Bernal and defective an icosaheda commonly foundy in laboratory a experiments. For example, one icosahedron (13 atoms, one at center) consists of 12 1551 clusters. The top and center atoms in an icosahedron linked with their shared five neighboring atoms might form a 1551 cluster. Because of the symmetry of the icosahedron, one icosahedron has 12 top atoms that would form 12 1551 clusters linked with center atom and five neighboring atoms respectively. If the central atom has 14 neighboring atoms, 12 of which are joined to the central atom by a 1551 cluster and two of which are joined to the central atom by a 1661 cluster, then they define a FK polyhedron. In the same way, other polyhedrons can be defined. A polyhedron consisting of some 1551, 1661, and/or 1441 clusters is called a defective icosahedron. An ideal icosahedron can be viewed as an important polyhedron in glass. As we know, glass not only has many of ideal icosahedra but also many defective icosahedra. The above analysis tells us that a 1551 cluster is the main part that forms an ideal icosahedron. During the cooling process there exists a competition between a local preference for an icosahedral structure and the global requirement of filling space; therefore, the system exhibits a growth of short-range icosahedral order until it is limited near the glass transition by frustration effects. The frustration comes from the difficulty in close packing with a perfect polyhedron in three-dimensional space. Various clusters in glass justly meet the demand of close packing during the glass formation. Therefore, a suitable proportion of the cluster is an important factor in glass formation. We argue that all icosahedra and defective icosahedra interpenetrate and share faces with other icosahedra and defective icosahedra during the glass formation. It can be concluded that both favorable energy and the smallest distortion for the 1551 cluster lead to its having the largest population in glass. Therefore, the bond energies, which are directly related to chemical short-range order, together with the geometrical constraint, play important roles in the local structures of glass. We concluded that the physical picture of the metallic glass is a disordered entanglement with a many icosahedra

Liquids an usually prepared by melting solids. Therefore, some microstructures of crystals such as 1421, 1422, 1661, and 1441 clusters would be kept in liquids. On the other hand, liquids contain many fivefold symmetrical structures such as 1551 and 1541 clusters not found in crystals.

VI. CONCLUSION

We perform molecular-dynamics simulations to study the transition from supercooled-liquid to solid (glass and crystal) cobalt. The MD simulation can be applied to determine Ω and E for rapidly quenched metallic liquids. Our simulation revealed a number of features of the freezing for a supercooled metallic liquid through a cooling process. It now appears that the transition from a supercooled liquid to a crystal is a first-order-like transition, and is a discontinuous transition in structure. The transition from a supercooled liquid to a glass is a continuous transition in structure. The splitting of the second peak of the PCF is due to the presence of icosahedron-type clusters and is further confirmed by existence of 1551 bonded pairs in glass. Our simulation reveals that glass formation requires a dynamical process at a proper cooling rate. Various clusters and their correlated motion can play very important roles in the transition from a supercooled liquid to a solid (glass and crystal). We suggest that there are not only internal relations but also certain differences between liquid and glass. During the process of the supercooled-liquid to crystal transition, the 1551-, 1541-, and 1431-type clusters convert to 1421 and 1422 atomic bonded pairs, which are characteristic of some stable crystalline structure. The above analysis tells us that the physical picture of the structure of metallic glass is a disordered entanglement with many lot of icosahedra.

ACKNOWLEDGMENTS

L.H. and W.G. would like to acknowledge support from the Natural Science Foundation of China, Grant Nos. 29890210, 50071028. This work was also supported in part by the Natural Science Foundation of Shandong province, Grant No. L2000F01.

*To whom correspondence should be addressed. Email address: wangqun@nju.edu.cn

[1] M. J. Mandell and J. P. Mctague, J. Chem. Phys. **64**, 3699 (1976).
[2] M. J. Mandell and J. P. Mctague J. Chem. Phys. **66**, 3070 (1977).
[3] P. J. Steinhardt, D. R. Nelson, and M. Ronchetti, Phys. Rev. B **28**, 784 (1983).
[4] D. H. Li, R. A. Moore, and S. Wang, J. Chem. Phys. **89**, 4309 (1988).
[5] H. Nakano, D. W. Qi, and S. Wang, J. Chem. Phys. **90**, 1871 (1989).
[6] D. W. Qi and S. Wang, J. Non-Cryst. Solids **135**, 73 (1991).
[7] J. Lu and D. W. Qi, Phys. Lett. A **157**, 283 (1991).
[8] D. W. Qi, J. Gryko, and S. Wang, J. Non-Cryst. Solids **127**, 306 (1991).
[9] W. Jin, R. K. Kalia, and P. Vashishta, Phys. Rev. B **50**, 118 (1994).
[10] B. Coluzzi, G. Parisi, and P. Verrocchio, Phys. Rev. Lett. **84**, 306 (2000).
[11] R. S. Liu, D. W. Qi, and S. Wang, Phys. Rev. B **45**, 451 (1992).
[12] S. K. Mitra, M. Amini, and D. Fincham, R. W. Hockney, Philos. Mag. **43**, 365 (1981).
[13] S. K. Mitra, Philos. Mag. **47**, L63 (1983).
[14] R. L. Mozzi and B. E. Warren, J. Am. Ceram. Soc. **2**, 164 (1969).
[15] S. Tsuneyuki, H. Aoki, and M. Tsukada, Phys. Rev. Lett. **64**, 776 (1990).
[16] S. K. Lai, S. Wang, and K. P. Wang, J. Chem. Phys. **87**, 599 (1987).
[17] S. E. Tsay, Phys. Rev. B **48**, 5945 (1993).
[18] F. H. Stillinger and R. A. Laviolette, Phys. Rev. B **34**, 5136 (1986).
[19] M. S. Watanabe, and K. Tsumuraya, J. Chem. Phys. **87**, 4891 (1987).
[20] C. S. Hsu and A. Rahman, J. Chem. Phys. **71**, 4974 (1979).
[21] M. Tanemura, Y. Hiwatari, H. Matsuda, T. Ogawa, N. Ogita, and A. Ueda, Prog. Theor. Phys. **58**, 1079 (1977).
[22] J. N. Cape, J. L. Finney, and L. V. Woodcock, J. Chem. Phys. **75**, 2366 (1981).
[23] R. D. Mountain and P. K. Basu, J. Chem. Phys. **78**, 7318 (1983).
[24] R. D. Mountain and A. C. Brown, J. Chem. Phys. **80**, 2730 (1984).
[25] C. C. Hsu and A. Rahman, J. Chem. Phys. **70**, 5234 (1979).
[26] M. W. Finnis and J. E. Sinclaire, Philos. Mag. A **50**, 45 (1984).
[27] M. S. Daw and M. I. Baskes, Phys. Rev. Lett. **50**, 1285 (1983).
[28] F. Gao and D. J. Bacon, Philos. Mag. A **67**, 275 (1993).
[29] G. J. Ackland, S. J. Wooding, and D. J. Bacon, Philos. Mag. A **71**, 553 (1995).
[30] G. J. Ackland, G. Tichy, V. Vitek, and M. W. Finnis, Philos. Mag. A **56**, 735 (1987).
[31] G. J. Ackland and M. W. Finnis, Philos. Mag. A **54**, 301 (1986).
[32] G. J. Ackland and R. Thetford, Philos. Mag. A **56**, 15 (1987).
[33] G. J. Ackland and V. Vitek, Phys. Rev. B **41**, 10 324 (1990).
[34] M. Igarashi, M. Khantha, and V. Vitek, Philos. Mag. B **63**, 603 (1991).
[35] D. Brown and J. H. R. Clare, Mol. Phys. **51**, 1243 (1984).
[36] W. G. Hoover, A. J. C. Ladd, and B. Moran, Phys. Rev. Lett. **48**, 1818 (1982).
[37] G. J. Martyna and M. L. Klein, J. Chem. Phys. **97**, 2635 (1992).
[38] D. J. Evans, J. Chem. Phys. **78**, 3297 (1983).
[39] F. H. Stillinger and T. A. Weber, Phys. Rev. A **25**, 978 (1982).
[40] F. H. Stillinger and R. A. Laviolette, Phys. Rev. B **34**, 5136 (1986).
[41] H. Jonsson and H. C. Anderson, Phys. Rev. Lett. **60**, 2295 (1988).
[42] W. C. Swope and H. C. Anderson, Phys. Rev. B **41**, 7042 (1990).
[43] J. P. Rose and R. S. Berry, J. Chem. Phys. **96**, 517 (1992).
[44] M. P. Allen and D. J. Tildesley, *Computer Simulation of Liquids* (Clarendon, Oxford, 1987).
[45] W. Jin, R. K. Kalia, P. Vashishta, and J. P. Rino, Phys. Rev. B **50**, 118 (1994).
[46] J. D. Honeycut and H. C. Anderson, J. Phys. Chem. **91**, 4950 (1987).
[47] H. Jonsson and H. C. Andersen, Phys. Rev. Lett. **60**, 2295 (1988).
[48] M. Kimura and F. Yonezawa, in *Topological Disorder in Condensed Matter*, edited by F. Yonezawa and T. Ninomiya (Springer, Berlin, 1983).
[49] P. A. Egelstaff, *An Introduction to the Liquid State* (Academic, New York, 1967).
[50] Y. Waseda, *The Structure of Non-crystalline Metals, Liquids and Amorphous Solids* (McGraw-Hill, New York, 1980).